

Suspension Design of Formula Racing Vehicle with Roll Independent Control Function



Zhe Liu, Zhonghao Li, Guanrong Chen, Shihao Jia, Mengjian Tian, and Da Wang

Abstract With an electric formula racing vehicle as the research object in the paper, a suspension design method with independent roll control function was introduced, and the conclusion that the suspension has different damping requirements in ride conditions and roll conditions was drawn. Compared with traditional vehicles without heave shock absorbers, this type of suspension realizes the decoupling of stiffness and damping in the heave and roll conditions, and different damping characteristics of the vehicles are obtained in ride conditions and roll conditions by adjusting the heave shock absorbers and inboard shock absorbers separately, to improve the vehicle attitude control and steering response. The effectiveness of the design was verified by simulation in the vehicle dynamics simulation software VI-Car Real Time.

Keywords Racecar · Suspension · Formula student · Heave absorber · Roll damper

1 Introduction

Handling stability is a main design goal of racing vehicle suspension, of which stiffness matching is an important technical issue in suspension design. In order to realize the decoupling of suspension line stiffness and angular stiffness, and to serve the needs of racing vehicle setup and aerodynamic design, the heave spring mechanism that only works in heave and pitch conditions has been widely used [1–3] (Fig. 1).

Similar to the stiffness, the line damping and angular damping of the suspension are coupled, so it is particularly important to calculate the damping separately under different working conditions [4]. Previously, Berman [5] conducted quantitative analysis and research on the vehicles equipped with heave shock absorbers, and concluded the conclusion that the heave shock absorbers can improve the pitch angles of vehicles without affecting the wheel center rate, but failed to give a specific physical model and calculation process.

Z. Liu · Z. Li · G. Chen · S. Jia · M. Tian · D. Wang (✉)
College of Automotive Engineering, Jilin University, Changchun 130022, Jilin, China
e-mail: wangda_gspeed@jlu.edu.cn

© The Author(s), under exclusive license to Springer Nature Singapore Pte Ltd. 2022
China Society of Automotive Engineers (eds.), *Proceedings of China SAE Congress 2020: Selected Papers*, Lecture Notes in Electrical Engineering 769,
https://doi.org/10.1007/978-981-16-2090-4_3

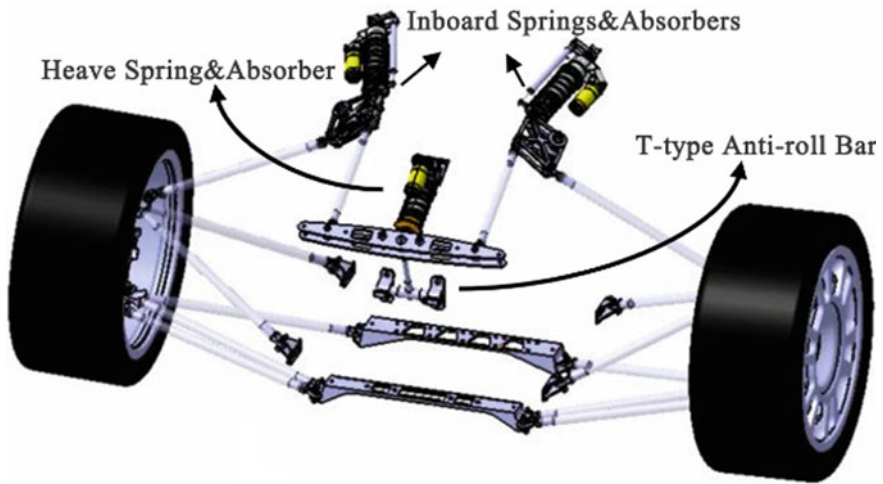


Fig. 1 The suspension equipped with heave shock absorber

There is currently no systematic calculation process regarding dynamics design and development of racing vehicles equipped with heave shock absorbers. In this paper, the roll damping and total ride damping of vehicles were calculated by establishing a simplified 1/2 vehicle roll model and a simplified 1/2 vehicle model.

2 Dynamics Design of Suspension Without Heave Shock Absorber

2.1 Ride Rate Matching with Ride Damping

The ride rate matching with the ride damping starts from the selection of a chassis natural frequency target of the vibration system, and after the stiffness and damping analysis and calculation, the process with the most suitable spring stiffness and motion ratio was finally selected. The flow chart can be seen in Fig. 2.

From Fig. 3, according to the analysis results of the aerodynamic sensitivity to racing vehicle in a straight driving condition with a speed of 15 m/s, it can be known that the negative lift level of the pitch angle in the range of plus or minus 1 degree is more significant, so the target with a steady-state pitch angle of racing vehicle not over plus or minus 1 degree was determined.

Based on the previous design experience, the front and rear chassis natural frequencies are determined to be 5.0 Hz and 4.7 Hz respectively.

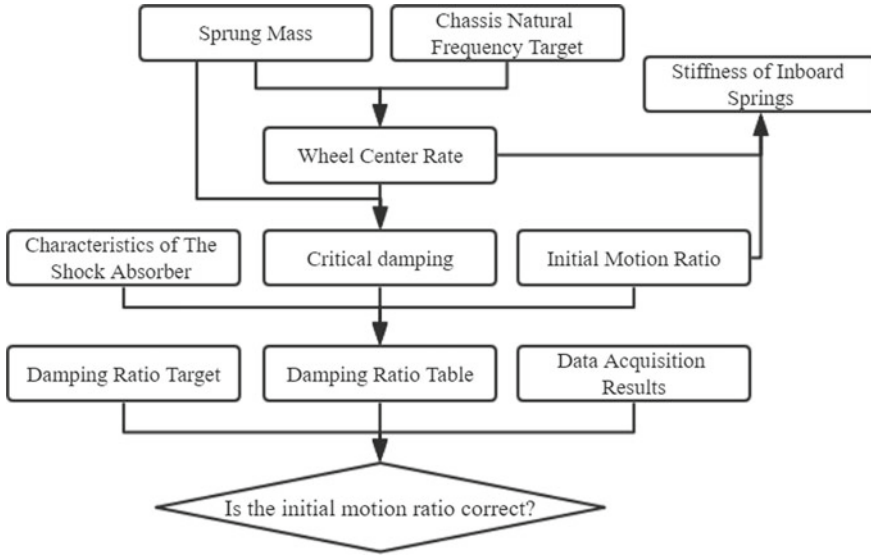
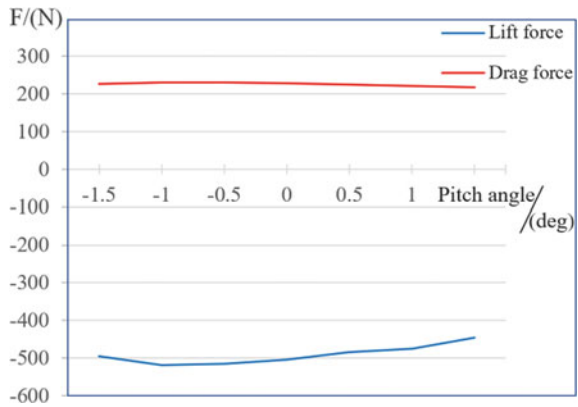


Fig. 2 Flow chart of suspension stiffness matching with damping

Fig. 3 Aerodynamic sensitivity of vehicle under 15 m/s straight driving condition



$$f_s = \frac{1}{2\pi} \sqrt{\frac{K_w}{\frac{m_s}{2}}} \tag{1.1}$$

wherein, f_s is the chassis natural frequency (Hz); m_s is the sprung mass of a shaft (kg); K_w is the wheel center rate (N/m).

After the chassis natural frequency target was determined, the wheel center rate of the front and rear suspension $K_{w,f}$, and $K_{w,r}$ was calculated based on the front and rear sprung mass according to formulas (1.2) and (1.3):

$$\begin{aligned}
K_{w_f} &= 4\pi^2 f_{-f}^2 \times \frac{m_{s_f}}{2} / 1000 \\
&= 57.4 \text{ N/mm}
\end{aligned} \tag{1.2}$$

$$\begin{aligned}
K_{w_r} &= 4\pi^2 f_{-r}^2 \times \frac{m_{s_r}}{2} / 1000 \\
&= 63.1 \text{ N/mm}
\end{aligned} \tag{1.3}$$

Then, according to the front and rear sprung mass, the ride critical damping C_{c_f} and C_{c_r} of the front and rear suspension can be calculated according to formulas 1.4 and 1.5:

$$\begin{aligned}
C_{c_f} &= 2\sqrt{K_{w_f} \times \frac{m_{s_f}}{2} \times 1000} \\
&= 3652.1 \text{ N s/m}
\end{aligned} \tag{1.4}$$

$$\begin{aligned}
C_{c_r} &= 2\sqrt{K_{w_r} \times \frac{m_{s_r}}{2} \times 1000} \\
&= 4274.6 \text{ N s/m}
\end{aligned} \tag{1.5}$$

The suspension motion ratio is defined as the ratio of wheel jump displacement to spring displacement. According to the previous season experience, the initial motion ratio is 1.10 for the front suspension and 1.09 for the rear suspension.

In this study, a special shock absorber with four-way damping coefficient was selected and used. Table 1 shows the characteristics of the shock absorber damping coefficient obtained through self-experiment or the shock absorber indicator diagram provided by the shock absorber manufacturer. The high-speed and low-speed damping can be separately adjusted by this shock absorber. The adjustment effect of low-speed damping between 0 and 0.1 m/s is obvious, and the adjustment effect of high-speed damping between 0.1 and 0.25 m/s is also obvious [6]. The low-speed damping requirements of racing vehicles were mainly studied in the paper.

The data in the table refer to the relationship between the damping coefficient of the shock absorber on each setpoint and the piston speed.

According to Table 1, according to formulas (1.6), the ride damping ratio of the shock absorber at different speeds and on varying setpoints can be obtained, and then a distribution table for the ride damping ratio of the inboard shock absorbers can be available.

$$\zeta = \frac{C}{M_R^2 \cdot C_c} \tag{1.6}$$

wherein, ζ is the damping ratio; M_R is the motion ratio of inboard springs (the ride spring on each wheel); C is the damping coefficient of the shock absorber on each wheel (N·s/m).

Table 1 Characteristics of the shock absorber

| Damping coefficient (N·s/m) | | Damper piston velocity (mm/s) | | | |
|-----------------------------|----------|-------------------------------|----------|-----------|--------|
| Low speed compression | Setpoint | 25 | 50 | 75 | 100 |
| | 1 | 680 | 420 | 400.00 | 420 |
| | 2 | 760 | 680 | 733.33 | 750 |
| | 3 | 960 | 980 | 1160.00 | 1260 |
| | 4 | 1720 | 1980 | 2120.00 | 2350 |
| | 5 | 2680 | 3520 | 3546.67 | 3620 |
| | 6 | 5720 | 5880 | 5093.33 | 4630 |
| Low speed rebound | 7 | 14,920 | 9240 | 6946.67 | 5810 |
| | 7 | - 12,520 | - 7520 | - 5653.33 | - 4680 |
| | 6 | - 4120 | - 4760 | - 4040.00 | - 3660 |
| | 5 | - 1880 | - 2160 | - 2506.67 | - 2690 |
| | 4 | - 1200 | - 1280 | - 1626.67 | - 1830 |
| | 3 | - 840 | - 820 | - 826.67 | - 880 |
| | 2 | - 560 | - 440 | - 480.00 | - 470 |
| 1 | - 520 | - 340 | - 320.00 | - 320 | |

Figures 4 and 5 show the data acquisition results of the real vehicle endurance race, intercepting the displacement velocity of the shock absorber under typical working conditions such as pylon course slalom driving. From the previous race season’s motion ratio, the wheel jump speed can be deduced, and the last column gives out the shock absorber speed of this race season calculated based on the initial motion ratio of the race season [7].

It can be seen from the figure that the wheel jump speed is within the range of 30–70 mm/s where wheels are not subjected to high speed excitation.

The choice of damping ratio is a trade-off between response time and overshoot. The design range of racing vehicle’s damping ratio is usually 0.65–0.70 [8], in which the response speed is higher than the critical damping and the overshoot is small.

Combining the above analysis results and the damping ratio target, the scenario when the shock absorber speed is 25–75 mm/s was mainly considered. According to Table 2, the adjustment ranges of the ride compression damping ratio of the front and rear suspensions are: 0.095–3.376 and 0.079–2.938 respectively; the adjustment ranges of the ride rebound damping ratio of the front and rear suspensions are 0.072–2.833 and 0.063–2.465 respectively.

In order to better alleviate the impact and recover the posture more quickly, the rebound damping required by the racing vehicle is usually bigger than the compression damping [8], so the fifth setpoint of compression damping and the sixth setpoint of rebound damping are used in the end. It can be seen that the damping adjustment range at the motion ratio covers the design goals. Hence it is concluded that the initial motion ratio is reasonable.

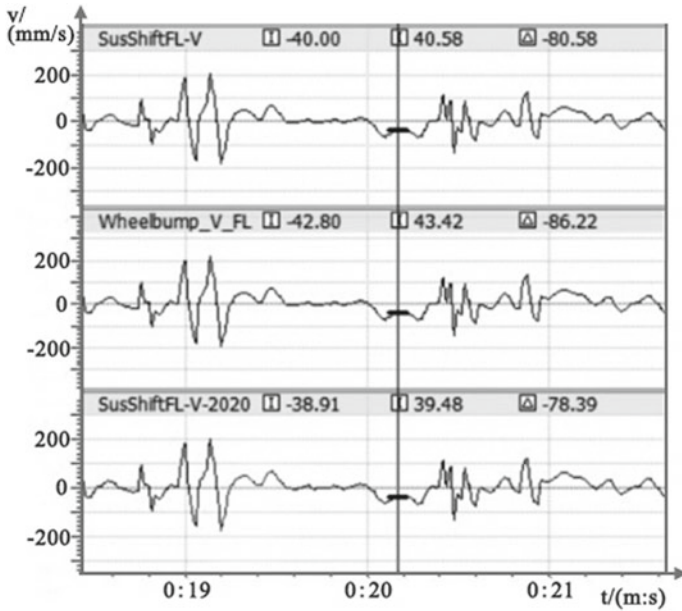


Fig. 4 Data of shock absorber and wheel displacement entering a corner

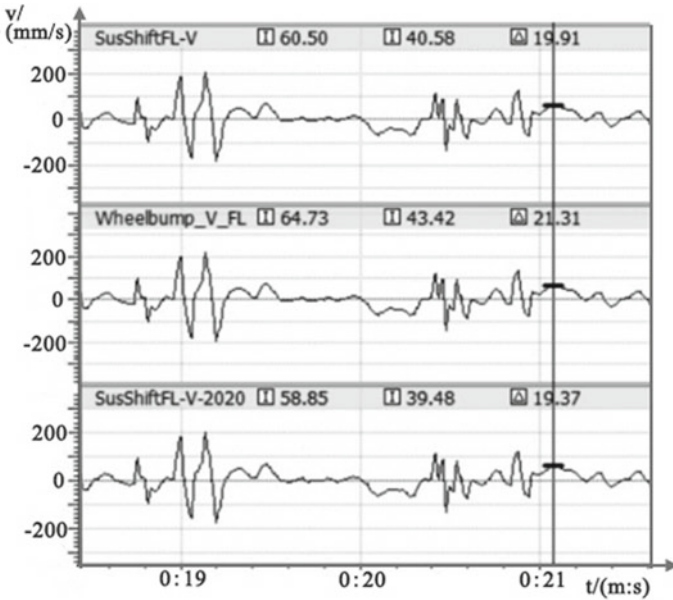


Fig. 5 Data of shock absorber and wheel displacement exiting a corner

Table 2 Ride damping ratio distribution of the inboard shock absorbers

| Ride damping ratio | | Setpoint | Damper Piston Velocity(mm/s) | | | |
|--------------------|-----------------------|----------|------------------------------|---------|---------|---------|
| | | | 25 | 50 | 75 | 100 |
| Front suspension | Low speed compression | 1 | 0.154 | 0.095 | 0.091 | 0.095 |
| | | 2 | 0.172 | 0.154 | 0.166 | 0.170 |
| | | 3 | 0.217 | 0.222 | 0.263 | 0.285 |
| | | 4 | 0.389 | 0.448 | 0.480 | 0.532 |
| | | 5 | 0.607 | 0.797 | 0.803 | 0.819 |
| | | 6 | 1.294 | 1.331 | 1.153 | 1.048 |
| | | 7 | 3.376 | 2.091 | 1.572 | 1.315 |
| | Low speed rebound | 7 | - 2.833 | - 1.702 | - 1.279 | - 1.059 |
| | | 6 | - 0.932 | - 1.077 | - 0.914 | - 0.828 |
| | | 5 | - 0.425 | - 0.489 | - 0.567 | - 0.609 |
| | | 4 | - 0.272 | - 0.290 | - 0.368 | - 0.414 |
| | | 3 | - 0.190 | - 0.186 | - 0.187 | - 0.199 |
| | | 2 | - 0.127 | - 0.100 | - 0.109 | - 0.106 |
| | | 1 | - 0.118 | - 0.077 | - 0.072 | - 0.072 |
| Rear suspension | Low speed Compression | 1 | 0.134 | 0.083 | 0.079 | 0.083 |
| | | 2 | 0.150 | 0.134 | 0.144 | 0.148 |
| | | 3 | 0.189 | 0.193 | 0.228 | 0.248 |
| | | 4 | 0.339 | 0.390 | 0.417 | 0.463 |
| | | 5 | 0.528 | 0.693 | 0.698 | 0.713 |
| | | 6 | 1.126 | 1.158 | 1.003 | 0.912 |
| | | 7 | 2.938 | 1.819 | 1.368 | 1.144 |
| | Low speed rebound | 7 | - 2.465 | - 1.481 | - 1.113 | - 0.922 |
| | | 6 | - 0.811 | - 0.937 | - 0.796 | - 0.721 |
| | | 5 | - 0.370 | - 0.425 | - 0.494 | - 0.530 |
| | | 4 | - 0.236 | - 0.252 | - 0.320 | - 0.360 |
| | | 3 | - 0.165 | - 0.162 | - 0.163 | - 0.173 |
| | | 2 | - 0.110 | - 0.087 | - 0.095 | - 0.093 |
| | | 1 | - 0.102 | - 0.067 | - 0.063 | - 0.063 |

The stiffness of the inboard springs was calculated according to formula (1.7). Because the spring pounds available on the market are fixed integers, in order to ensure the expected wheel center rate, it is necessary to find the spring with the stiffness closest to the calculated value, and then re-substitute into the motion ratio formula for correction.

$$M_R = \sqrt{\frac{K_s}{K_w}} \tag{1.7}$$

wherein, K_s is the spring stiffness (N/m); K_w is the wheel center rate (N/m).

2.2 Spring Selection

2.2.1 Inboard Springs

Based on the experience of previous race season, the chassis natural frequency was set to 3.5 for the front suspension and 3.2 for the rear suspension when no heave spring was added. Of which the motion ratio of inboard springs remains the same as the initial one, that is, it is 1.10 for the front suspension and 1.09 for the rear suspension.

According to formula (1.7), the stiffness of the inboard spring is calculated as 34.01 N/mm (194.4 lb/in) for the front suspension and 34.76 N/mm (198.6 lb/in) for the rear suspension. Because most of the spring poundage customized on the market are integers, the inboard spring poundage of the front and rear wheels are both 200 lb/in. According to this spring poundage, the motion ratio of inboard springs is back calculated as: 1.116 for the front suspension and 1.094 for the rear suspension. Compared with the initial selection result, the motion ratio is fit.

2.2.2 Heave Spring

The heave spring is the third spring connected in parallel with two inboard springs. Its characteristic is that it only works in the heave and pitch conditions but does not work in the roll condition. From the spring parallel formula and formula (1.8), the following can be deduced:

$$K_w = K_{w1} + \frac{K_{w3}}{2} = \frac{K_{s1}}{M_{R1}^2} + \frac{K_{s3}}{2M_{R3}^2} \quad (1.8)$$

wherein, K_{w1} is the wheel center rate provided by the inboard springs (N/mm); K_{w3} is the wheel center rate provided by the heave spring (N/mm); K_{s1} is the stiffness of the inboard springs (N/mm); K_{s3} is the stiffness of the heave spring (N/mm); M_{R1} is the motion ratio of the inboard springs; M_{R3} is the motion ratio of the heave spring.

The motion ratio of the heave spring primarily selected is 1.04 for the front suspension and 0.98 for the rear suspension. The poundage of the heave spring can be calculated as 78.80 N/mm (450.3 lb/in) for the front suspension and 77.80 N/mm (444.6 lb/in) for the rear suspension., so the poundage of the front and rear heave springs are both 450 lb/in. In the dynamics design of the three-spring suspension without heave shock absorber, no careful correction is required for the motion ratio of the heave spring.

2.3 Angular Stiffness Matching with Roll Damping

2.3.1 Target Selection of Roll Gradient and Stiffness Calculation

The roll gain selected for the 2019 racing season is $0.65^\circ/\text{g}$. According to the analysis, it was found that Continental C16 tires have soft sidewalls and high tread stiffness. Under the condition of large lateral forces, the tires deform seriously, so the roll stiffness of the suspension should not be too high. In combination with the target that the steady-state roll angle set based on the results of aerodynamic sensitivity analysis does not exceed plus or minus 1.5° , the roll gain of $0.7^\circ/\text{g}$ is selected for the new race season.

According to formulas (1.9) and (1.10), the height of the sprung mass center h_s and the length of the roll arm h_{RM} (center of mass to roll axis distance) can be calculated:

$$\begin{aligned} h_s &= \frac{m \cdot h_{CG} - m_{u_f} \cdot R_{t_f} - m_{u_r} \cdot R_{t_r}}{m_s} \\ &= 0.288 \text{ m} \end{aligned} \quad (1.9)$$

$$\begin{aligned} h_{RM} &= h_s - \left(h_{RC_f} + (h_{RC_r} - h_{RC_f}) \left(1 - \frac{m_{s_f}}{m_s} \right) \right) \\ &= 0.252 \text{ m} \end{aligned} \quad (1.10)$$

wherein, m is the vehicle mass (kg); h_{CG} is the height of mass center (m); m_s is the sprung mass (kg); m_u is the unsprung mass (kg); R_t is the radius of tire load (m); h_{RC} is the height of roll center (m).

After that, the roll moment M_φ and the total roll angle stiffness K_φ when the lateral acceleration of the vehicle is a_y were calculated according to formulas (1.11) and (1.12):

$$M_\varphi = m_s \cdot a_y \cdot h_{RM} \quad (1.11)$$

$$\begin{aligned} K_\varphi &= \frac{M_\varphi}{\varphi} = \frac{m_s \cdot a_y \cdot h_{RM}}{RG \cdot \frac{a_y}{g}} \\ &= 920.969 \text{ N m}/^\circ \end{aligned} \quad (1.12)$$

wherein, a_y is the lateral acceleration (m/s^2); φ is the roll angle (deg); RG is the roll gain (deg/g), and “g” in this unit is the gravitational acceleration.

After that, the total load transfer LT under the condition of unit lateral acceleration was calculated according to formula (1.14) according to the average wheel track T_{ave} :

$$T_{ave} = \frac{T_{-f} + T_{-r}}{2} = 1.235 \text{ m} \quad (1.13)$$

$$\frac{LT}{a_y} = \frac{m \cdot h_{CG}}{T_{ave}} = 68.21 \text{ kg/g} \quad (1.14)$$

Theoretically, when the load transfer distribution of front and rear axle is equal to the axle load distribution, the steering characteristic is neutral. To ensure a certain initial understeer, when calculating the load transfer distribution, the load transfer distribution of front axle should be 5% more [9], so the load transfer of the front axle is calculated under the condition of unit lateral acceleration according to formula (1.15):

$$\frac{LT_{-f}}{a_y} = \frac{LT}{a_y} \times \left(\frac{m_{s-f}}{m_s} + 5\% \right) \quad (1.15)$$

When the vehicle runs with a lateral acceleration, the roll moment of the vehicle is equal to the sum of the roll moment caused by the centrifugal force of the sprung mass, the roll moment caused by the centrifugal force of the unsprung mass, and the counter moment of the suspension acting on the body. Thus according to the torque balance:

$$\begin{aligned} LT_{-f} \cdot T_{-f} &= K_{\varphi-f} \cdot RG \cdot \frac{a_y}{g} \\ &+ m_{s-f} \cdot a_y \cdot h_{RC-f} + m_{u-f} \cdot a_y \cdot R_{t-f} \end{aligned} \quad (1.16)$$

Therefore, the required roll stiffness $K_{\varphi-f}$ and $K_{\varphi-r}$ of the front and rear suspension can be calculated according to formulas (1.17) and (1.18):

$$\begin{aligned} K_{\varphi-f} &= \frac{g}{RG} \left(\frac{LT_{-f}}{a_y} \cdot T_{-f} - m_{s-f} \cdot h_{RG-f} - m_{u-f} \cdot R_{t-f} \right) \\ &= 486.38 \text{ N m}^\circ \end{aligned} \quad (1.17)$$

$$K_{\varphi-r} = K_{\varphi} - K_{\varphi-f} = 435.62 \text{ N m}^\circ \quad (1.18)$$

The analysis shows that the inboard springs are connected in parallel with the anti-roll bar and connected in series with the tires. According to the spring series/parallel formula, the formula (1.19) can be obtained:

$$\frac{1}{K_{\varphi}} = \frac{1}{K_{\varphi_s} + K_{\varphi_{arb}}} + \frac{1}{K_{\varphi_t}} \quad (1.19)$$

wherein, K_{φ_s} is the roll stiffness provided by the springs (N m[°]); $K_{\varphi_{arb}}$ is the roll stiffness provided by the anti-roll bar (N m[°]); K_{φ_t} is the roll stiffness provided by the tires (N m[°]).

Take the front suspension as an example, and calculate the roll stiffness $K_{\varphi_{s-f}}$ provided by the inboard springs according to formula (1.20):

$$\begin{aligned}
 K_{\varphi s_f} &= \frac{\pi}{180} \times \frac{K_{w1,2} \cdot T_{-f}^2}{2} \\
 &= 393.16 \text{ N m/}^\circ
 \end{aligned}
 \tag{1.20}$$

Calculate the roll stiffness $K_{\varphi t_f}$ provided by the front suspension tires according to formula (1.21):

$$\begin{aligned}
 K_{\varphi t_f} &= \frac{\pi}{180} \times \frac{K_{t_f} \cdot T_{-f}^2}{2} \\
 &= 1230.83 \text{ N m/}^\circ
 \end{aligned}
 \tag{1.21}$$

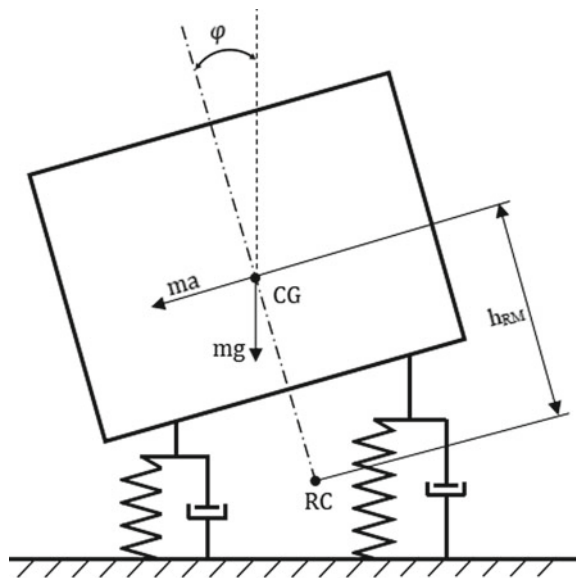
According to formula (1.22), the roll stiffness $K_{\varphi arb_f}$ provided by the front suspension anti-roll bar is calculated as:

$$\begin{aligned}
 K_{\varphi arb_f} &= \frac{1}{\frac{1}{K_{\varphi_f}} - \frac{1}{K_{\varphi t_f}}} - K_{\varphi s_f} \\
 &= 410.98 \text{ N m/}^\circ
 \end{aligned}
 \tag{1.22}$$

2.3.2 Calculation of Roll Damping

Take the front suspension as an example, and establish a simplified 1/2 vehicle roll model as shown in Fig. 6.

Fig. 6 Simplified 1/2 vehicle roll model



In the figure, CG is the position of mass center, and RC is the roll center. Taking the position shown in the figure as the origin, and it is positive around the angle φ counterclockwise; it can be obtained relying on the torque balance:

$$I_{RC} \cdot \varphi'' \approx I_{xx} \cdot \varphi'' = -C'_{roll\varphi} - K_{roll}\varphi$$

or

$$\varphi'' + \frac{C_{roll}}{I_{xx}}\varphi' + \frac{K_{roll}}{I_{xx}}\varphi = 0 \quad (1.23)$$

wherein, I_{RC} is the moment of inertia of the vehicle around the roll center axis (kg m^2); I_{xx} is the moment of inertia of the vehicle around the x axis ($\text{kg}\cdot\text{m}^2$); C_{roll} is the roll damping coefficient [$\text{N}\cdot\text{m}/(\text{rad}\cdot\text{s}^{-1})$]; K_{roll} is the tire-free roll stiffness ($\text{N}\cdot\text{m}/^\circ$).

Because the experimental data only has the vehicle's moment of inertia around the x axis, and the distance between the roll center axis and the ground is small, the approximate equation can be established. Formula (1.23) is the free vibration differential equation of the simplified roll model of the vehicle [10]. In order to solve it, set:

$$\varphi = e^{st} \quad (1.23a)$$

wherein, s is the undetermined constant, and after substituting it into formula (1.23), the following can be obtained:

$$\left(s^2 + \frac{C_{roll}}{I_{xx}}s + \frac{K_{roll}}{I_{xx}} \right) e^{st} = 0 \quad (1.23b)$$

It can be known that formula (1.23b) satisfies formula (1.23), that is, formula (1.23b) is the solution to formula (1.23), as long as there is:

$$s^2 + \frac{C_{roll}}{I_{xx}}s + \frac{K_{roll}}{I_{xx}} = 0 \quad (1.23c)$$

Formula (1.23c) is the characteristic equation of formula (1.23), with two roots s_1 and s_2 ; when the two roots are equal, the roll damping coefficient is the critical roll damping coefficient. Take the front suspension as an example:

$$\begin{aligned} K_{roll_f} &= K_{\varphi s_f} + K_{\varphi arb_f} \\ &= 804.14 \text{ N m}/^\circ \\ &= 46073.83 \text{ N m}/\text{rad} \end{aligned} \quad (1.24)$$

$$I_{xx_f} = I_{xx_13} \cdot K \cdot \frac{m_{s_f}}{m_s} - I_{xxu}$$

$$= 8.1700 \text{ kg m}^2 \tag{1.25}$$

wherein, $I_{xx_{13}}$ ($\text{kg}\cdot\text{m}^2$) is the measured moment of inertia along the x-axis of the racing vehicle in the season 2013; K is the mass ratio of the racing vehicle in this season to that in the season 2013. Relying on formulas (1.24) and (1.25), the critical damping coefficient $C_{c,roll}$ of the front suspension roll can be calculated:

$$C_{c,roll} = \sqrt{4I_{xx_{f}} \cdot K_{roll_{f}}} \\ = 1227.07 \text{ N m}/(\text{rad s}^{-1}) \tag{1.26}$$

Because the steady-state roll angle of the vehicle is controlled within $\pm 1.5^\circ$, and the tangent value of the roll angle is linear approximate to its radian value, there are formulas (1.27a, b)–(1.30). The roll damping ratio corresponding to the setpoint selected according to the design results of the inboard damping under the ride condition was calculated relying on formulas (1.27a, b) and (1.28) in Table 3.

$$\varphi \approx \tan \varphi = \frac{x_{s_{f1}} - x_{s_{fr}}}{T_{f} \cdot M_{R_{f}}} \tag{1.27a}$$

$$\varphi' = \frac{x'_{s_{f1}} - x'_{s_{fr}}}{T_{f} \cdot M_{R_{f}}} \tag{1.27b}$$

$$C_{roll} = \frac{(F_{c_{f1}} - F_{c_{fr}})M_{R_{f}} \cdot \frac{T_f}{2}}{\varphi'} \tag{1.28}$$

$$F_c = C \cdot v_s \tag{1.29}$$

$$\zeta_{roll} = \frac{C_{roll}}{C_{c,roll}} \tag{1.30}$$

wherein, x_s is the displacement of the inboard shock absorber (m); v_s is the piston speed of the inboard shock absorber (m/s); F_c is the damping force of the inboard

Table 3 Roll damping ratio distribution of the inboard shock absorbers

| Roll damping ratio | Damper piston velocity (mm/s) | Roll damping ratio | Compression setpoint | 4 | 5 |
|--------------------|-------------------------------|--------------------|----------------------|-------|-------|
| | | Rebound setpoint | | | |
| Front suspension | 25 | 6 | | 1.885 | 2.165 |
| | 50 | 6 | | 2.146 | 2.636 |
| Rear suspension | 25 | 6 | | 1.729 | 2.014 |
| | 50 | 6 | | 1.996 | 2.452 |

shock absorber (N); the subscripts f_l and f_r indicate “Left front” and “Right front” respectively. It can be seen from Table 3 that in the three-spring suspension without heave damping, the roll damping ratio is much larger than the target value 0.65–0.70 when the damping requirements of the ride condition are met, and there is obvious over damping. In other words, there is a contradiction in the damping required between the roll working condition and the ride condition.

3 Dynamic Design of Suspension with Heave Shock Absorber

3.1 Establishment of Simplified 1/2 Vehicle Model

3.1.1 Establishment of Simplified 1/2 Vehicle Model

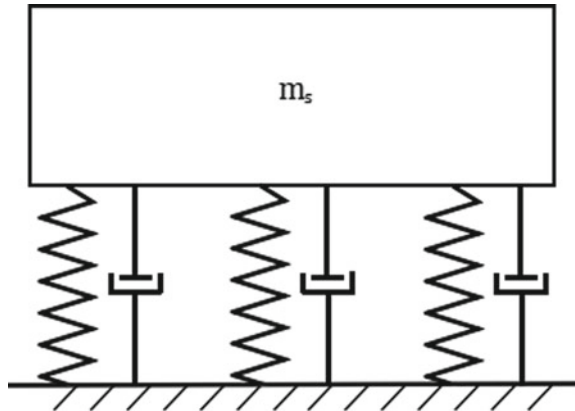
The heave shock absorber mechanism realizes the calculation of roll damping independently, but the pitch damping and ride damping of the vehicle are still partially coupled. In order to facilitate the research, the ride damping is mainly calculated, then the trade-off between the ride and pitch damping is achieved by tuning the inboard shock absorbers.

Taking the front suspension as an example, a simplified 1/2 vehicle model was established as shown in Fig. 7. The heave shock absorber in the middle is connected in parallel with the inboard shock absorber.

Taking the position shown in the figure as the origin and the displacement direction vertically downward as positive, the force balance can be obtained:

$$m_s \cdot x'' = -2C_{1,2} \cdot x' - C_3 \cdot x' - 2K_w \cdot x$$

Fig. 7 Simplified 1/2 vehicle model



or

$$x'' + \frac{(2C_{1,2} + C_3)}{m_s} x' + \frac{2K_w}{m_s} x = 0 \quad (2.1)$$

In order to distinguish them, wherein, $C_{1,2}$ is the damping coefficient of the inboard shock absorber (N·s/m); C_3 is the damping coefficient of the heave shock absorber (N·s/m). The total critical damping coefficient $C_{c,total}$ was calculated:

$$C_{c,total} = 2C_{c1,2} + C_{c3} = 2\sqrt{2m_s \cdot K_w} \quad (2.2)$$

wherein, $C_{c1,2}$ is the inboard ride critical damping coefficient (N·s/m); C_{c3} is the heave ride critical damping coefficient (N·s/m). From Eq. (1.6), the total ride damping ratio of the simplified 1/2 vehicle model vibration system can be calculated as:

$$\begin{aligned} \zeta_{total} &= \left(\frac{2C_{1,2}}{M_R^2} + \frac{C_3}{M_{R3}^2} \right) \cdot \frac{1}{C_{c,total}} \\ &= \zeta + \frac{\zeta_3}{2} \end{aligned} \quad (2.3)$$

$$\zeta_3 = \frac{C_3}{M_{R3}^2 \cdot C_{c3}} \quad (2.4)$$

wherein, M_{R3} is the heave spring motion ratio.

3.1.2 Matching with the Ride Damping of Heave Shock Absorber

From the analysis in 1–3 above, it can be concluded that the moment of inertia of the vehicle around the roll axis is low, so the demand for roll damping of the vehicle is less than that for ride damping. Thus, the idea concerning the damping of the heave shock absorber matching with the stiffness should start from the roll damping target, and after the inboard damping conversion and comparison, and the damping ratio and setpoint of the heave shock absorber can be obtained (Fig. 8).

In order to quickly attenuate the vibration in the roll condition, the damping ratio of the roll condition is primarily set as 0.65–0.7. Table 4 lists the roll damping ratio corresponding to the lower setpoint of the inboard shock absorber:

It can be seen from Table 4 that the distribution of damping ratio is relatively coherent, which caters to the relatively consistent characteristics of the damping coefficient of this shock absorber at low speeds and low setpoints. After comparison, the third setpoint of compression damping and the fourth setpoint of rebound damping were selected.

From Table 2 and 5 can be obtained for the ride damping ratio provided by the inboard shock absorber in the ride working condition when the roll damping requirements are met.

Fig. 8 Flow chart of suspension stiffness matching with heave damping

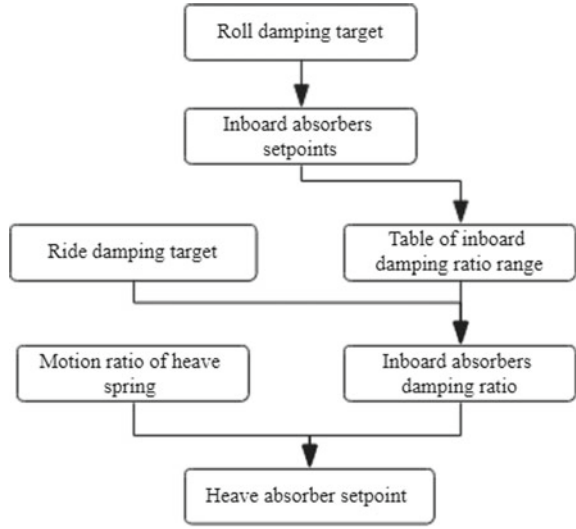


Table 4 Roll damping ratio distribution corresponding to low setpoints

| Roll damping ratio | Damper piston velocity (mm/s) | Roll damping ratio | | Compression setpoint | |
|--------------------|-------------------------------|--------------------|--|----------------------|-------|
| | | Rebound setpoint | | 2 | 3 |
| Front suspension | 25 | 3 | | 0.509 | 0.573 |
| | | 4 | | 0.624 | 0.688 |
| | | 5 | | 0.840 | 0.904 |
| | 50 | 3 | | 0.478 | 0.573 |
| | | 4 | | 0.624 | 0.719 |
| | | 5 | | 0.904 | 1.063 |
| Rear suspension | 25 | 3 | | 0.474 | 0.533 |
| | | 4 | | 0.580 | 0.640 |
| | | 5 | | 0.782 | 0.841 |
| | 50 | 3 | | 0.444 | 0.533 |
| | | 4 | | 0.580 | 0.669 |
| | | 5 | | 0.841 | 0.930 |

Table 5 Ride damping ratio distribution corresponding to low setpoints

| Ride damping ratio | | Setpoint | Damper piston velocity (mm/s) | |
|--------------------|----|----------|-------------------------------|----------|
| | | | 25 | 50 |
| Front sus. | LC | 3 | 0.2172 | 0.2218 |
| | LR | 4 | - 0.2716 | - 0.2897 |
| Rear sus. | LC | 3 | 0.1890 | 0.1930 |
| | LR | 4 | - 0.2363 | - 0.2520 |

Depending on Table 1, in case that the motion ratio of the heave spring on the front and rear suspensions was initially established according to formula (2.4), the ride damping ratio of the heave shock absorber at different speeds and different setpoints could be calculated, and then a distribution table for the ride damping ratio of the heave shock absorber was obtained.

According to the ride damping ratio provided by the heave shock absorber in Table 6, in combination with the ride damping ratio provided by the lower setpoint of the inboard shock absorber in Table 5, the distribution of the total ride damping ratio can be calculated according to formula (2.3).

From Table 7, the compression damping on the 4th–5th setpoint and the rebound damping on the 6th setpoint were finally determined for the front suspension heave shock absorber; the compression damping on the 5th setpoint and the rebound damping on the 6th setpoint were finally determined for the rear suspension heave shock absorber.

3.2 Simulation Verification

In this paper, the parametric simulation software VI-Car Real Time was used for simulation to verify the positive effect of the heave shock absorber on the lateral acceleration and yaw velocity of the racing vehicle in the composite racing track.

3.2.1 Establishment of Parametric Simulation Model

In simulation, Continental C16 tires were used in the vehicle model, and the tire model based on PAC2002 magic formula provided by the manufacturer was adopted.

As shown in Fig. 9, the front suspension is taken as an example. The suspension model of the racing vehicle was established in the multi-body dynamics software Adams car and its stiffness, spring motion ratio and other parameters were fitted [11].

After that, the suspension and steering model were exported through the VI-Car Real Time-plugin plug-in to generate a parametric model.

Table 6 Ride damping ratio distribution of the heave shock absorber

| Ride damping ratio | | Setpoint | Damper piston velocity (mm/s) | | | |
|--------------------|-----------------------|----------|-------------------------------|---------|---------|---------|
| | | | 25 | 50 | 75 | 100 |
| Front sus. | Low speed compression | 1 | 0.177 | 0.109 | 0.104 | 0.109 |
| | | 2 | 0.198 | 0.177 | 0.191 | 0.196 |
| | | 3 | 0.250 | 0.256 | 0.302 | 0.328 |
| | | 4 | 0.448 | 0.516 | 0.553 | 0.613 |
| | | 5 | 0.699 | 0.918 | 0.925 | 0.944 |
| | | 6 | 1.491 | 1.533 | 1.328 | 1.207 |
| | | 7 | 3.889 | 2.409 | 1.811 | 1.515 |
| | Low speed rebound | 7 | - 3.264 | - 1.960 | - 1.474 | - 1.220 |
| | | 6 | - 1.074 | - 1.241 | - 1.053 | - 0.954 |
| | | 5 | - 0.490 | - 0.563 | - 0.653 | - 0.701 |
| | | 4 | - 0.313 | - 0.334 | - 0.424 | - 0.477 |
| | | 3 | - 0.219 | - 0.214 | - 0.216 | - 0.229 |
| | | 2 | - 0.146 | - 0.115 | - 0.125 | - 0.123 |
| | | 1 | - 0.136 | - 0.089 | - 0.083 | - 0.083 |
| Rear sus. | Low speed compression | 1 | 0.166 | 0.102 | 0.098 | 0.102 |
| | | 2 | 0.185 | 0.166 | 0.179 | 0.183 |
| | | 3 | 0.234 | 0.239 | 0.283 | 0.307 |
| | | 4 | 0.419 | 0.482 | 0.516 | 0.572 |
| | | 5 | 0.653 | 0.857 | 0.864 | 0.882 |
| | | 6 | 1.393 | 1.432 | 1.241 | 1.128 |
| | | 7 | 3.634 | 2.251 | 1.692 | 1.415 |
| | Low speed rebound | 7 | - 3.050 | - 1.832 | - 1.377 | - 1.140 |
| | | 6 | - 1.004 | - 1.160 | - 0.984 | - 0.892 |
| | | 5 | - 0.458 | - 0.526 | - 0.611 | - 0.655 |
| | | 4 | - 0.292 | - 0.312 | - 0.396 | - 0.446 |
| | | 3 | - 0.205 | - 0.200 | - 0.201 | - 0.214 |
| | | 2 | - 0.137 | - 0.107 | - 0.117 | - 0.114 |
| | | 1 | - 0.127 | - 0.083 | - 0.078 | - 0.078 |

Parametric simulation of the vehicle was conducted in VI-Car Real Time, by use of the provided electric formula racing vehicle model, and the tires, suspension, steering and other subsystems were imported. The vehicle model parameters used in the simulation are shown in Table 8 VI-Car Real Time.

Table 7 Total ride damping ratio distribution

| Total ride damping ratio | | Inboard absorbers setpoints | Heave absorber setpoint | Damper piston velocity (mm/s) | |
|--------------------------|----|-----------------------------|-------------------------|-------------------------------|---------|
| | | | | 25 | 50 |
| Front sus. | LC | 3 | 4 | 0.441 | 0.480 |
| | | | 5 | 0.567 | 0.681 |
| | LR | 4 | 5 | - 0.517 | - 0.571 |
| | | | 6 | - 0.809 | - 0.910 |
| Rear sus. | LC | 3 | 4 | 0.399 | 0.434 |
| | | | 5 | 0.515 | 0.622 |
| | LR | 4 | 5 | - 0.465 | - 0.515 |
| | | | 6 | - 0.738 | - 0.832 |

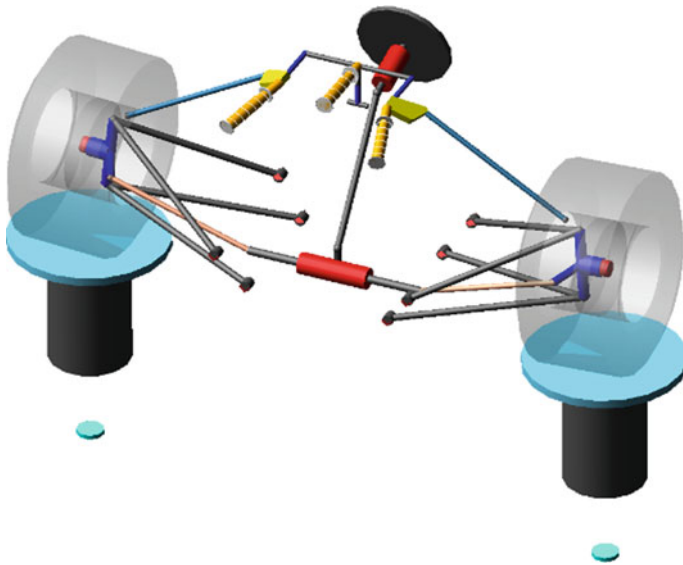


Fig. 9 The front suspension model equipped with heave shock absorber

3.2.2 Simulation Results and Analysis

In the simulation of the racing track with a course of 1195.70 m, the lap time of the racing vehicle equipped with heave shock absorbers was 60.10 s, and that of the racing vehicle without heave shock absorbers was 60.87 s. The 800–860 m typical pylon course slalom track was intercepted for analysis (Fig. 10).

For a better comparison, Fig. 11 shows the curve of vehicle roll angle in response to the course under the pylon course slalom condition. It can be known that because the

Table 8 Vehicle model parameters

| Parameter Name | Symbol | Value | Unit |
|---------------------------------------|-----------------|---------|-------------------|
| Mass | m | 305 | kg |
| Wheelbase | L | 1575 | mm |
| Mass Center Height | h | 280 | mm |
| Dist. from mass Center to Front Shaft | a | 866.25 | mm |
| Dist. from mass Center to Rear Shaft | b | 708.75 | mm |
| Moment of inertia Around the X Axis | I _{xx} | 36.245 | kg·m ² |
| Moment of inertia around the Y Axis | I _{yy} | 122.765 | kg·m ² |
| Moment of inertia Around the Z Axis | I _{zz} | 143.768 | kg·m ² |

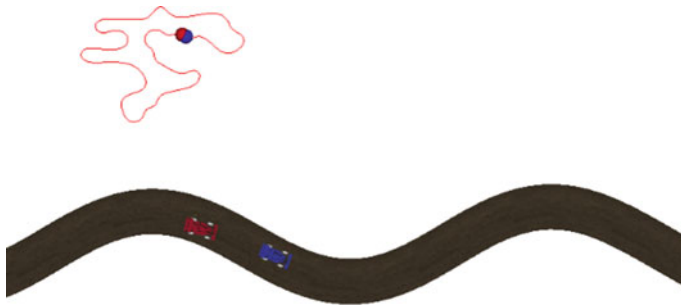
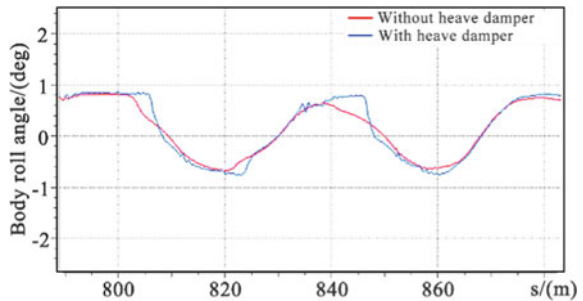


Fig. 10 Pylon course slalom track

Fig. 11 Comparison of roll angle response



roll stiffness matching with damping is more reasonable, the roll vibration attenuation speed of the vehicle equipped with pitch shock absorbers is higher.

Figures 12 and 13 show the comparison curves of the vehicle's lateral acceleration and yaw rate in response to the course in this working condition respectively. It can be known that when the vehicle is equipped with heave shock absorbers, the peak value of roll acceleration and yaw rate is larger, and their establishment speeds are higher.

Fig. 12 Comparison of lateral acceleration response

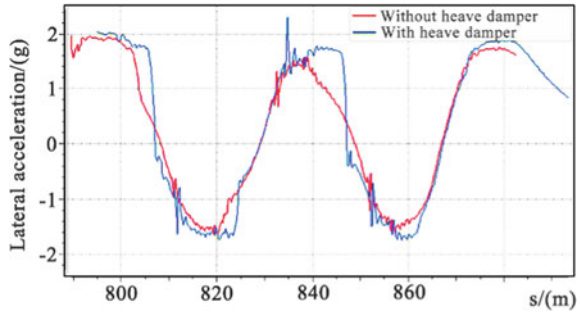
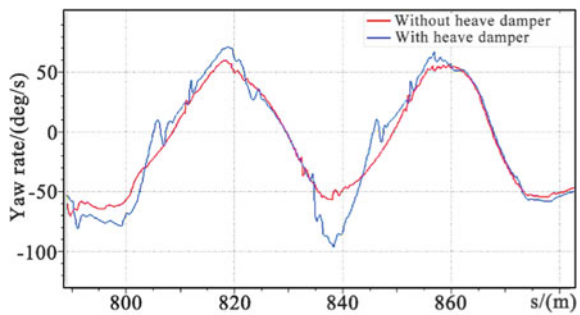


Fig. 13 Comparison of yaw rate response



4 Conclusion

In this paper, by establishing the simplified 1/2 vehicle roll model and the simplified 1/2 vehicle model, the vehicle roll damping and the total ride damping of the vehicle equipped with heave shock absorber were calculated respectively, and were simulated in VI-Car Real Time. The following conclusions can be drawn in accordance with the calculation and simulation results:

1. For the vehicles without heave shock absorbers, the front suspension as an example: when the ride low-speed compression damping ratio is 0.4–0.8, and the low-speed rebound damping ratio is 0.9–1.1, the roll low-speed damping ratio is 1.9–2.6, the over-damping situation is obvious. Therefore, there is a contradiction in the damping required for the roll condition and the ride condition.
2. The ride damping and roll damping of the vehicles equipped with heave shock absorbers were decoupled. Taking the front suspension as an example, when the ride low-speed compression damping ratio is 0.4–0.7, and the low-speed rebound damping ratio is 0.5–0.9, the roll low-speed damping ratio is 0.6–0.7.
3. After a vehicle simulation on the composite racing track with a course of 1195.70 m, the lap time of the vehicle with heave shock absorbers is 0.77 s higher than that without heave shock absorbers; in the pylon course slalom

condition, the average increase in the amplitude of the vehicle's roll angle is only 0.072° ; the average increase in the yaw rate is 12.36%.

References

1. 马芳武, 李金杭,等. 一种抗俯仰汽车悬架系统[P].中国专利:201610894612.9
2. 张光宇. FSAE赛车悬架设计与调校[D].上海: 同济大学, 2017
3. 马芳武, 李金杭,等. 一种抗俯仰汽车悬架系统[P].中国专利 2020(08):79-82
4. Rouelle C (2018) Formula student 101. *Race Car Eng* 28(4):58-60
5. Berman R (2016) Optimisation of a three spring and damper suspension
6. Gacka SP, Doherty CG (2006) Design analysis and testing of dampers for a formula SAE race car. SAE Paper 2006-01-3641
7. Segers J (2008) Analysis techniques for racecar data acquisition. SAE International 2008
8. Seward D (2014) Race car design
9. Milliken WF, Milliken DL (1995) Race car vehicle dynamics
10. 张义民, 李鹤. 机械振动学基础. 高等教育出版社 (2010)
11. 陈军. MSC.ADAMS 技术与工程分析实例. 中国水利水电出版社 (2008)